Polymerization of Myosin from Smooth Muscle of the Calf Aorta†

Joseph Megerman‡ and Susan Lowey*

ABSTRACT: Myosin from smooth muscle of the calf aorta has been found to be similar to rabbit skeletal muscle myosin in molecular weight, sedimentation coefficient, and amino acid composition. When dialyzed at low ionic strength, it also forms polymers that exist in equilibrium with the "monomer", the position of this equilibrium being sensitive to ionic strength, pH, and hydrostatic pressure. The self-association reactions for smooth muscle myosin differ, however, from those observed for skeletal muscle myosin in several ways: (1) aorta myosin polymerizes at a higher ionic strength to form a smaller polymer; (2) between pH 6 and 8, only one polymer boundary is observed; (3) the result of varying total protein concentration on the myosin–polymer equilibrium cannot be analyzed by the Gilbert theory for a simple two-species system, as was possible with skeletal myosin. This more complex polymerization behavior may be related to differences in the mode of assembly between smooth and skeletal muscle myosin.

The contractile process in striated and vertebrate smooth muscles is thought to similarly depend on the interaction of thick and thin filaments (Needham, 1971). But the structure of the thick filaments in the two types of muscle may be significantly different, even though myosin is the dominant component in both. In skeletal muscle, a bipolar structure results from myosin molecules oriented in opposite directions from either end of a central bare zone (Huxley, 1969). The structure of myosin filaments in vertebrate smooth muscles is less well-known because of their greater lability, and the reduced order of the filament matrix, which for many years delayed their visualization by electron microscopy and X-ray diffraction [for a review, see Somlyo et al. (1977)]. Two basic configurations have been proposed: the bipolar structure described for striated muscle thick filaments (Ashton et al., 1975), and a "face-polar" structure that lacks a central bare zone, but has a single and opposite orientation of myosin cross bridges along the entire length of two sides of the filament (Small & Squire, 1972).

The study of filaments formed in vitro from purified myosin has provided supplementary information on thick filament structures. When the ionic strength of a solution of myosin from rabbit skeletal muscle is lowered, bipolar filaments markedly similar in morphology to those found in intact muscle are formed (Huxley, 1963; Kaminer & Bell, 1966). Their assembly appears to be initiated by the anti-parallel association of myosin tails to establish the central bare zone, and growth then proceeds by the parallel addition of myosin, thus maintaining the overall bipolar configuration of the filament. The in vitro polymerization of vertebrate smooth muscle myosin, however, has not resolved the ambiguity relating to the structure of the native thick filament. Either bipolar filaments were formed that were too short to correspond to those thought to exist in vivo (Hanson & Lowy, 1964; Shoenberg, 1969; Kaminer, 1969; Wachsberger & Pepe, 1974) or longer filaments lacking central bare zones were formed, whose morphology suggested the association of only anti-parallel units (Sobieszek, 1972, 1977; Sobieszek & Small, 1972; Craig & Megerman, 1977). These have been interpreted either as having a "side-polar" structure that can be reconciled with the "face-polar" filaments of intact muscle (Craig & Megerman, 1977) or as having a helical structure in which "adjacent rows of bridges have oppositely polarized cross bridges" (Hinssen et al., 1978).

These different modes of assembly are not readily associated with known differences in the myosins of striated and vertebrate smooth muscles. Both myosins have similar physical properties, as determined by measurements of sedimentation, viscosity, and amino acid composition (Lowey & Cohen, 1962; Huriaux et al., 1965; Wachsberger & Kaldor, 1971; Gröschel-Stewart, 1971; Frederiksen, 1979). They contain heavy and light chains (Murphy & Megerman, 1977) and can be cleaved into heavy and light meromyosins (Cohen et al., 1961; Huriaux, 1965; Bárány et al., 1966). Smooth muscle myosin is more readily extracted at low ionic strength and is more difficult to isolate from actin (Murphy & Megerman, 1977; Hinssen et al., 1978), but these properties may reflect the presence of contaminants and not be inherent in the purified myosins (Ruegg, 1971). The enzymatic functions of the two myosins are also similar, linking ATPase activity to the presence of calcium and the dissociation of actomyosin. They do differ in how this function is controlled: in smooth muscle, the regulatory protein is probably a light chain of myosin and is thus located on the thick filament (Bremel, 1974; Sobieszek & Small, 1976; Aksoy et al., 1976; Chacko et al., 1977), while in striated muscle, it is a subunit of the thin filament (Ebashi et al., 1969). Also, in the absence of actin, the ATPase activity of smooth muscle myosin increases with ionic strength while the reverse is true of skeletal muscle myosin (Megerman, 1974). However, since the rod portion of smooth muscle myosin by itself generates the side-polar morphology (Craig & Megerman, 1977), these enzymatic differences between skeletal and smooth muscle myosins are not sufficient to account for the observed differences in thick filament structures.

We therefore compared the processes by which the two myosins polymerize in vitro in the hope of establishing a basis for explaining the formation of different types of filaments. The analytical ultracentrifuge and electron microscope were used in a manner parallel to the studies by Josephs & Harrington (1966, 1967, 1968) on skeletal muscle myosin, and in some cases, their experiments were duplicated with both proteins to allow for meaningful comparisons. While the two myosin systems demonstrated a similar dependence of polym-

† From the Rosenstiel Basic Medical Sciences Research Center, Brandeis University, Waltham, Massachusetts 02254. *Received March 18, 1980; revised manuscript received November 14, 1980.* Supported by National Institutes of Health Postdoctoral Fellowship HL-02278 to J.M. and by grants from the National Institutes of Health (5 R01 AM17350), the National Science Foundation (PCM 782 2710), and the Muscular Dystrophy Association to S.L.

‡ Present address: Vascular Research Laboratory, Massachusetts General Hospital, Boston, MA 02114.

0006-2960/81/0420-2099$01.25/0 © 1981 American Chemical Society

erization on ionic conditions and hydrostatic pressure, a notable difference in the equilibrium relationship between myosin and polymer was found. The equilibrium distribution of smooth muscle myosin was most consistent with the simultaneous presence of numerous polymers of different size that perhaps form a link between the monomer and the fully grown thick filament. The unusual features of this distribution may perhaps be related to the side-polar type of structure observed by electron microscopy (Craig & Megerman, 1977; Hinssen et al., 1978). We present these physicochemical studies as a step toward the goal of clarifying thick filament structure in nonstriated muscle as well as in nonmuscle cells.

Materials and Methods

Preparation of Smooth Muscle Myosin. Calf aortas were collected within minutes of the animals' death in an ice-cold physiological salt solution consisting of 4.7 mM KCl, 0.135 M NaCl, 1.2 mM $NaHPO_4$, 0.02 mM EDTA, and 9 mM imidazole, pH 7.4 (Megerman, 1974). Unless otherwise stated, all subsequent operations were performed at 4 °C. The aortas were sliced longitudinally, carefully stripped of their adventitia, washed thoroughly in distilled water to remove traces of blood, ground twice in a household meat grinder, and weighed. On the average, 40 aortas gave 800 g of minced media. The mince was placed in 2.5 mL/g extraction buffer [25 mM potassium inorganic phosphate (KP_i) and 0.5 mM DTT, pH 7.0], homogenized in a Sorvall Omnimixer, left standing for 2–3 h, and then centrifuged for 20 min at 8000 rpm (Sorvall GS-3 rotor). The supernatant pH was adjusted to 6.4 by the slow addition of 1 N HCl, KCl was added to 0.15 M, and actomyosin was allowed to precipitate overnight. Under these conditions, all of the extracted myosin was precipitated; when either more or less KCl was added, the precipitation of myosin was incomplete. Typical concentrations of protein in the extract were from 4 to 6 mg/mL.

The separation of myosin from actin constitutes the single greatest problem in the purification of smooth muscle myosin. It is well-known that conditions which readily dissociate skeletal muscle actomyosin, i.e., high salt concentration and the presence of Mg, ATP, and a Ca-chelating agent, are considerably less effective in the case of smooth muscle actomyosin (Murphy & Megerman, 1977; Hinssen et al., 1978). As determined by analytical ultracentrifugation, not much actomyosin was dissociated in the presence of 2 mM MgATP, with or without Ca. More, though not all, of the actomyosin could be dissociated in the presence of 10 mM Mg or 1 mM EDTA (no Mg), again with 2 mM ATP.

A workable compromise, similar to that used by others (Hamoir & Gaspar-Godfroid, 1964; Megerman, 1974), was to use 0.6 M KCl, 10 mM KP_i, 10 mM MgATP, and 0.5 mM DTT, pH 8. The actomyosin precipitate was dissolved in buffered 3 M KCl and dialyzed without Mg or ATP. These were added to the desired concentration just prior to centrifugation for 30 min at 50 000 rpm (Beckman 60 Ti rotor) to remove large aggregates. The supernatant protein concentration was determined with the biuret procedure, adjusted to $\leq$2 mg/mL with MgATP-containing buffer, and then fractionated with ammonium sulfate. Starting with a low protein concentration appears to be critical, since the fractionation of more concentrated samples was not successful. Tris buffer, which interferes with the biuret determination, was therefore not used at this stage, despite its greater buffering capacity at pH 8 when compared to phosphate. Solid ammonium sulfate was added to 33% saturation, precipitating much of the actin and some of the myosin. After the precipitate was removed by centrifugation, a significant amount of actin still remained in the supernatant. With skeletal muscle actomyosin, practically all of the actin and almost none of the myosin are precipitated under these conditions. The greater solubility of smooth muscle actin in ammonium sulfate may be related to its greater tendency to depolymerize (Megerman & Murphy, 1975). The supernatant was then adjusted to pH 6 by adding 1 M KH_2PO_4, ammonium sulfate was added to 66% saturation, and the solution was allowed to stand for 30 min. The insoluble protein was again collected by centrifugation, for 30 min at 20 000 rpm (Beckman 21 rotor), which produced two zones of precipitate—a typical sediment, and a floating zone that coated the upper wall of the tube after careful decantation. The lower density portion was presumably the result of air having been trapped during precipitation. Sodium dodecyl sulfate ($NaDodSO_4$) gel electrophoresis showed that the two zones were equal in protein composition, and they were combined. The large amount of ammonium sulfate that is required reflects the higher solubility of smooth muscle myosin. In the high-salt buffer used, $\sim$0.26 mg/mL remains soluble at 50% ammonium sulfate saturation, compared to less than 0.04 mg/mL soluble skeletal muscle myosin under identical conditions.

With the volume of the precipitate kept to a minimum, the sample was dialyzed against 0.6 M KCl, 0.015 M KP_i, 1 mM MgATP, and 0.5 mM DTT, pH 7.5, to remove ammonium sulfate prior to gel filtration chromatography. At this stage, the sample consisted of 40–60% myosin and 20–10% actin, respectively, the rest being tropomyosin and unidentified contaminants, depending on the preparation. Chromatography was performed on 4% agarose (Sepharose 4B, Pharmacia) equilibrated with the dialysis buffer, using a 5 × 90 cm column equipped with flow adaptors. The sample volume was limited to 3% of the bed volume, and protein concentration was adjusted to give an optical density of no more than 6 units at 280 nm (estimated to be about 10 mg/mL for this heterogeneous sample). A small amount of DNP-glycine was added as a convenient marker, and the sample was cleared of particulates by centrifuging 5 min at top speed in the bench-top clinical centrifuge. The column was eluted with 0.6 M KCl, at 60 mL/h, by using a peristaltic pump, and 18-mL fractions were collected. With the exception of ionic strength, the composition of the elution buffer is immaterial, since it never comes into contact with the eluted protein. For retardation of bacterial growth during the subsequent storage of the column, this buffer included 0.02% sodium azide. The elution profile was monitored at 280 nm with an ISCO Model UA-5 absorbance monitor. A typical scan contained three peaks: (1) actomyosin, (2) pure myosin, and (3) low molecular weight proteins, including depolymerized actin and tropomyosin.

The myosin-containing fractions were pooled, the pH was adjusted to about 6.2 with 1 M KH_2PO_4, and solid ammonium sulfate was added to 70% saturation. After the solution was allowed to stand for 30 min, it was centrifuged for 1 h at 20 000 rpm. The two zones of the precipitate (sediment and float) were combined and dialyzed extensively against 0.6 M KCl, 0.025 M KP_i, 1 mM EDTA, and 0.5 mM DTT, pH 7, in which the myosin was stored on ice. The concentration of the final product was typically between 8 and 12 mg/mL. This relatively low concentration was partly due to the high density of 70% saturated ammonium sulfate, which made packing of the precipitate difficult.

The yield of purified myosin was approximately 25 mg per 100 g wet weight of media, which is less than 25% of the total myosin extractable at high ionic strength. Major losses are due to (1) the low ionic strength extraction, which leaves

behind about half the total myosin (Megerman, 1974); (2) the incomplete separation of actin and myosin by MgATP, resulting in their coprecipitation during ammonium sulfate fractionation; and (3) the high solubility of smooth muscle myosin, which precludes a large fraction of myosin in dilute solutions from being recovered. For instance, the concentration of the pooled column fractions was typically about 0.5 mg/mL, and about 0.1 mg/mL myosin remained in solution after precipitation by ammonium sulfate. Although more myosin could be precipitated by dialysis in low salt (e.g., 10 mM KP_i, pH 6, or 0.1 M KCl), the resultant myosin often exhibited irreversible aggregation, so that this procedure was avoided. When necessary, aggregates could usually be removed by dialyzing the proteins against 0.075 M KP_i, 5 mM EDTA, and 0.5 mM DTT, pH 7.5, and centrifuging 60 min at 30000 rpm (Beckman 40 rotor). If this procedure was insufficient, the protein was chromatographed on a DEAE-Sephadex column equilibrated in the same buffer and eluted with a KCl gradient. In 0.15 M KP_i and 10 mM EDTA, which is the usual buffer for chromatographing skeletal muscle myosin on DEAE-Sephadex (Richards et al., 1967; Godfrey & Harrington, 1970), aorta myosin will pass through the column unretarded.

Preparation of Skeletal Muscle Proteins. Myosin from rabbit leg and back muscles was typically prepared by the method of Holtzer & Lowey (1959) and chromatographed on DEAE-Sephadex (Godfrey & Harrington, 1970). In one preparation, the contractile proteins were extracted in 0.6 M KCl, 25 mM KP_i, and 0.5 mM DTT, pH 7, and all subsequent steps were those normally used to make aorta myosin. No functional differences were observed in the polymerization of skeletal muscle myosins produced by these two methods. Rabbit actin was the generous gift of Dr. S. S. Margossian and was prepared by the method of Spudich & Watt (1971).

Protein Determination. The concentration of pure skeletal myosin was measured by the absorbance at 280 nm, corrected for light scattering by subtraction of the absorbance at 340 nm, by using the extinction coefficient $\epsilon_{1\%}^{280} = 5.2$ (Godfrey & Harrington, 1970). Similar determinations were made for pure aorta myosin, with $\epsilon_{1\%}^{280} = 4.82$ as determined by the micro-Kjeldahl procedure, using DEAE-Sephadex-purified protein and assuming 16% for the nitrogen fraction. Heterogeneous samples were analyzed by the biuret method (Gornall et al., 1949; Megerman, 1974).

Molecular Weight Determination. The molecular weight of myosin was determined from high-speed meniscus depletion equilibrium experiments (kindly performed by Dr. W. F. Stafford, III) by using Rayleigh interference optics. An Yphantis 30-mm 6-channel cell was used, with initial protein concentrations of 0.4, 0.13, and 0.04 mg/mL. Equilibrium was established at a speed of 10000 rpm after 72 h at 5 °C. Window distortion was corrected for by subtraction of the fringe pattern obtained from a run by using the same cell (without being dismantled) filled with solvent in all channels. The photographic plates were scanned with a flat-bed densitometer. Fringe displacements were determined by the Fourier-transform method of DeRosier et al. (1972) and analyzed by the computer program of Roark & Yphantis (1969). A partial specific volume of 0.728 mL/g was assumed.

Viscosity. Viscosity measurements were made with Ostwald-type viscometers at 20 and 5 °C, with careful attention paid to the preparation of clean and fiber-free solutions, as described previously (Lowey et al., 1969). Flow times for solvent at the two temperatures were about 130 and 180 s, respectively, and for protein solutions they ranged from 20 to 120 s above solvent times.

Amino Acid Analyses. A 1 mg/mL solution of DEAE-chromatographed myosin was prepared for analysis by exhaustive dialysis against 0.1 N acetic acid and freeze-dried. Portions of 100 μg were hydrolyzed in 0.5 mL of constant-boiling HCl (Pierce) in evacuated tubes at 110 °C for 24, 48, and 72 h. Cysteine was converted to cysteic acid by performic acid oxidation, and the sample was hydrolyzed for 24 h only. Samples (20 μg) were analyzed on a Durrum D500 analyzer (kindly provided by Dr. L. A. Steiner). The data presented are averaged values from at least 12 analyses (four runs for each hydrolysis time), except for cysteine, and for serine and threonine which are values extrapolated to zero time.

Gel Electrophoresis. Protein samples and gels were prepared according to the method of Weber & Osborn (1969). The gels were electrophoresed at 8 mA/tube, fixed and stained overnight in 0.025% Coomassie blue in 25% methanol–7% acetic acid, and destained by diffusion. Densitometry was performed on a Joyce-Loebl densitometer, and peak areas were measured by planimetry.

The linear range of stain uptake was determined for light chains on 10% acrylamide gels and for heavy chains on 5% gels. The results for light and heavy chains were linear to at least 25 or 4 μg of myosin, respectively. The use of actin as a marker, which stained to nearly the same degree on both sets of gels, permitted the stoichiometry of light and heavy chains to be determined. The amount of nonmyosin contamination was determined by loading up to 40 μg on 7% gels, and comparing the staining of contaminants to that of light chains.

Enzymatic Activity. ATPase assays were carried out at 25 °C by using 0.2 mg of myosin in a total volume of 2 mL. Ionic conditions were established as described by Chacko et al. (1977): for Ca-dependent activation, 0.5 M KCl, 20 mM Tris, pH 7.5, 2 mM ATP, and 10 mM $CaCl_2$; for K(EDTA)-dependent activation, 2 mM EDTA was substituted for the calcium; for Mg-dependent activation, 0.02 M KCl, 10 mM imidazole, pH 7.2, 1 mM ATP, and 1.6 mM $MgCl_2$. When actin activation was being tested, myosin and actin were first combined at high ionic strength and then adjusted to the final conditions specified for the Mg-containing assay. Reactions were initiated by the addition of ATP and terminated by adding 1 mL of 15% trichloroacetic acid. Inorganic phosphate was measured by the method of Fiske & Subbarow (1952).

Polymerization of Myosin. All myosin that was used in polymerization experiments was determined to be free of aggregates by velocity sedimentation in 0.6 M KCl, 25 mM KP_i, 1 mM EDTA, and 0.5 mM DTT, pH 7. Except where otherwise noted, all polymers were formed during dialysis against several hundred volumes of low ionic strength buffer, over a period of at least 24 h. This procedure was used to approximate uniformity in the rates of polymerization, which were known to affect the size and amount of polymer formed (Craig & Megerman, 1977). Sample volumes were typically about 1 mL, which was sufficient to allow for a determination of protein concentration as well as analysis in the ultracentrifuge. Myosin was diluted with the above high salt buffer to desired concentrations before being placed in dialysis against 2 mM phosphate (for pH 6 or 7), or 2 mM veronal buffer (pH 8), in addition to 1 mM EDTA, 0.5 mM DTT, and KCl. The substitution of phosphate for veronal at pH 8 produced no significant difference; veronal was preferred for its greater buffering capacity near pH 8, and because it had been the buffer used by Josephs & Harrington (1966) in their study on skeletal muscle myosin polymerization. The highest value of pH was limited to 8.0, rather than 8.3 as when skeletal

myosin was studied, because of a tendency for aorta myosin to denature at higher pH.

The dialyzed protein was placed into chilled Corex (Sorvall) centrifuge tubes (15-mL capacity) and spun 1 min at 7500 rpm to remove particulates. One aliquot was then loaded into a chilled analytical centrifuge cell, and another was saved for protein determination. At no time were the samples subjected to a temperature greater than 10 °C unless warming was desired. Protein concentrations were determined by UV absorbance, in duplicate. All samples were diluted (usually 1:1) with 3 M KCl to completely depolymerize such components as might cause an increase in light scattering. Low values of absorbance at 340 nm verified that depolymerization was essentially complete.

All analytical centrifuge experiments were carried out in the Beckman Model E at 5 °C, 20000 rpm, except where noted. Photographs were taken with schlieren and/or interference optics, using metallographic or spectroscopic plates, respectively. The asymmetrical slit was used when both optical systems were recorded. Two boundaries were typically observed of which the slower sedimented with a velocity typical of myosin monomer. Although this boundary could well have included species larger than monomer, the two boundaries will for simplicity be referred to as the "monomer" and "polymer" boundaries. Monomer concentrations were determined from photographs taken well after the slower boundary was established, and when the faster boundary was distinct from the slower. Polymer concentration was assumed to be the difference between total and monomer concentrations. In early experiments, monomer concentrations were determined by planimetry of the slower peak, using 8 × 10 in. photographic enlargements of the schlieren pattern. In these experiments only, 30-mm synthetic boundary cells were used when the total protein concentration was <2 mg/mL; in all other cases, 12-mm cells were used. Using the 30-mm cells permitted an accurate delineation of the slower boundary when diffusion might otherwise have been a problem with the less concentrated samples (Josephs & Harrington, 1966). In most experiments, monomer concentrations were determined from fringe counts, assuming 4 fringes mg^{-1} mL^{-1}. As discussed under Results, when the total protein concentration was high, the concentration between the slower and fast-moving boundaries did not remain constant but rather showed an increase with increasing radius. This behavior was seen with both aortic and skeletal muscle myosin. The rate of this increase was approximately constant, and the monomer concentration was defined at the point where the constant slope was tangent to the slower boundary. Appropriate corrections were made for radial dilution. All plates were analyzed on a Nikon microcomparator. Whenever possible, all polymerized samples were analyzed within 2 days, to minimize the possible effects of aging on the polymerization equilibrium. When schlieren and/or interference patterns were obtained, the two-hole rotor (AN-D) was used with one cell containing a (positive) wedge window. When only interference photographs were required, three samples could be examined in the four-hole rotor (AN-F) by using three cells, two of which contained a wedge window, one positive and one negative.

Light Scattering. Light scattering of protein solutions at a 90° angle was measured in a Perkin-Elmer MPF-44 fluorescence spectrophotometer at 600 nm, 10 °C (Wegner, 1976). For minimization of contributions from large fibrous aggregates, all samples were cleared by centrifugation for 20 min at 10000 rpm (Sorvall SS-34 rotor) immediately before being introduced into the fluorometer cell.

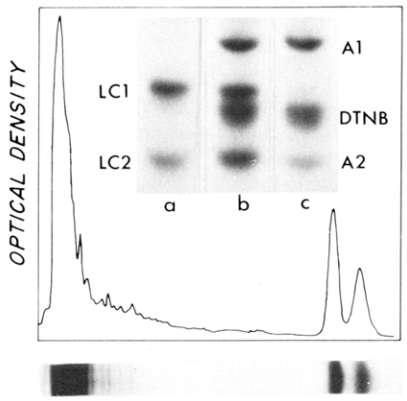

FIGURE 1: Electrophoresis of 30 μg of purified aorta myosin on a 7% polyacrylamide–0.1% $NaDodSO_4$ gel, along with its densitometer tracing (migrating from left to right). Note the absence of detectable actin. Inset: Comparison of light chains of smooth and skeletal muscle myosins on 10% $NaDodSO_4$–polyacrylamide gels (transport shown downward). (a) Aorta myosin, 50 μg; (b) mixture of samples of (a) plus (c); (c) skeletal myosin, 50 μg.

Electron Microscopy. Electron micrographs were obtained by Dr. R. Craig as previously described (Craig & Megerman, 1977). A drop of filament suspension was placed on a carbon film coated grid, fixed with 2.5% glutaraldehyde in 0.1 M sodium cacodylate, pH 7, and negatively stained with 1% uranyl acetate. Grids were examined in a Philips EM 301 electron microscope.

Results

Monomeric Aorta Myosin. The composition of calf aorta myosin is similar to that of other smooth muscle myosins: $NaDodSO_4$ gels exhibit one heavy chain (HC) and two light chains (LC1, LC2; Figure 1). The molecular weights of these chains were estimated by electrophoresis of samples of aorta and skeletal muscle myosin on the same sodium dodecyl sulfate–polyacrylamide gel.

The heavy chains of these two myosins could not be distinguished on 5% gels, nor could the most mobile light chains (LC2) be distinguished on 10% gels (Figure 1). However, LC1 was visibly less mobile than the 5,5′-dithiobis(2-nitrobenzoic acid) (DTNB) light chain of skeletal myosin. By use of 200000, 25000, 18000, and 16000 for the molecular weights of skeletal myosin subunits (Lowey & Risby, 1971), values of 200000, 20000, and 16000 were assigned to HC, LC1, and LC2 of calf aorta myosin. From integrated densitometer tracings of stained gels, LC1 and LC2 account for 14.0% and 8.6% of the total weight of myosin, giving a molar ratio of 1.3 for the two light chains. Since the uptake of stain by different proteins may be nonuniform (Potter, 1974), and allowing for experimental variability, the stoichiometry of the myosin subunits is probably 1:1:1. Skeletal muscle actin, which was used to control for differences in stain uptake between the 5% and 10% gel systems, absorbed twice as much stain per weight of applied protein as did aorta myosin. This 2-fold difference is considerably higher than the 7% difference in the staining of smooth muscle actin vs. myosin reported by Tregear & Squire (1973).

All samples that were tested for ATPase activity were active in the presence of Ca or EDTA, at high ionic strengths. Typical values in μmol of P_i/(mg·min) were 0.14 (Ca) and 0.45 (EDTA) at 25 °C. These assays were usually performed about 10 days after the calves were killed. No sample tested at any point during the purification procedure displayed measurable activity in the presence of Mg at low ionic strength, nor did skeletal actin activate purified aorta myosin. This lack

Table I: Amino Acid Composition of Myosins from Smooth and Skeletal Muscles (Expressed as Residues per 10^5 g)

amino acid	calf aorta	bovine carotid[a]	hog aorta[b]	chicken gizzard[c]	human uterus[d]	horse esophagus[e]	rabbit skeletal[f]
Asx	90	89	88	89	94	103	85
Thr	40	40	45	44	46	38	44
Ser	38	38	40	47	42	33	39
Glx	181	183	167	166	179	178	157
Pro	13	15	20	25	23	17	22
Gly	34	34	41	48	40	28	40
Ala	76	74	78	76	80	77	78
Cys	7.0	9.1	7.4	9.9		8.4	8.8
Val	37	39	33	41	40	38	43
Met	25	23	24	20	18	21	23
Ile	33	33	28	36	45	33	42
Leu	99	93	92	87	96	99	81
Tyr	15	14	18	16	17	14	20
Phe	29	28	34	27	34	27	29
His	12	12	16	14	17	12	16
Lys	87	85	87	88	96	76	92
Arg	52	49	55	48	51	43	43

[a] Huriaux et al. (1965). [b] Fredericksen (1979). [c] Barany et al. (1966). [d] Gröschel-Stewart (1971). [e] Yamaguchi et al. (1970). [f] Lowey & Cohen (1962).

of actin activation was presumably due to the absence of a kinase which is required for smooth muscle actomyosin activity (Dabrowska et al., 1979) or to its having been rendered inactive.

The sedimentation coefficients of aortic and skeletal muscle myosins, in 0.6 M KCl, 0.025 M KP_i, 1 mM EDTA, and 0.5 mM DTT, pH 7, were indistinguishable when the two proteins were analyzed in the same run: $s^0_{20,w} = 5.8$ at 60000 rpm and 20 °C. Samples of the former appeared homogeneous even after sedimentation for over an hour. By equilibrium sedimentation, the molecular weight of smooth muscle myosin was determined to be 510000 ± 5000 when samples were obtained directly from the gel filtration column. The second virial coefficient was calculated to be $(3.36 \pm 0.05) \times 10^{-2}$ L/g, and a slight tendency toward the formation of dimers was noted, with an apparent dimerization constant of 0.4 ± 0.2 L/g. This value was independent of protein loading concentration, implying good sample homogeneity. In contrast, a measurable amount of higher aggregates was found in samples taken after precipitation with ammonium sulfate, though such aggregates were rarely detectable by velocity sedimentation, using schlieren optics. The viscosity of aortic myosin was consistently around 2.5 dL/g (three preparations), or slightly greater than that found with skeletal muscle myosin (Lowey et al., 1969), which could reflect the presence of aggregates.

Amino acid analysis is given in Table I, which includes, for comparison, the amino acid compositions of several other smooth muscle myosins, as well as rabbit skeletal myosin. Our result is virtually identical with that obtained with bovine carotid myosin (Huriaux et al., 1965) but differs in some respects from skeletal myosin (Lowey & Cohen, 1962).

Polymerization of Aorta Myosin. (1) Dependence on Ionic Conditions. The polymerization of myosin from aortic smooth muscle is governed by pH and ionic strength in a manner similar to that described by Josephs & Harrington (1966) for skeletal muscle myosin. As the ionic strength is decreased from 0.6 M KCl, wherein myosin is primarily a monomer, some monomer polymerizes to form a single fast sedimenting boundary. We will use the phrase "single polymeric species" operationally to imply that the molecular dimensions of all aggregates are sufficiently similar to make differences indistinguishable by velocity sedimentation. When the ionic strength is lowered still further, more polymer is formed at the expense of monomer, until a concentration of KCl is reached below which all detectable myosin exists in polymer form. These limits of the region of monomer–polymer equilibrium vary with pH (Table II) and reflect the distribution of species at a given protein concentration, as determined by the equilibrium constant. Although the size of the aggregate formed is also a function of pH, becoming larger with decreasing pH, each set of conditions nevertheless produces a single polymeric species (Figure 2). This is in sharp contrast with the skeletal myosin system, wherein monomer is in equilibrium with several different polymeric species (distin-

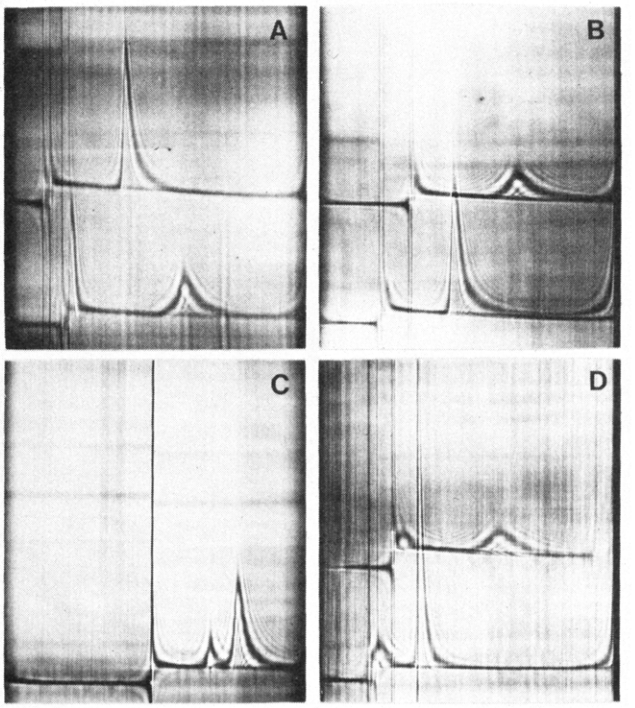

FIGURE 2: Examples of the apparent "two-species system" formed by aorta myosin at different values of pH and ionic strength. (A) 3.5 mg/mL total protein concentration at pH 6, 0.2 M KCl (upper trace) and 0.3 M KCl (lower trace); (B) 0.2 M KCl, pH 7, with 2.4 (upper) and 4.2 (lower) mg/mL protein; (C) 0.2 M KCl, pH 7, with 1 mg/mL protein; (D) 0.2 M KCl, pH 8, with 1.7 (upper) and 4.8 (lower) mg/mL protein. Cells were 12 mm, except for (C) which was obtained with a 30-mm synthetic boundary cell. Note the formation of the slow boundary at the meniscus in (A), (B), and (D), and that only two "species" were apparent in all systems examined. Note also the seemingly complete separation of the two boundaries at these low protein concentrations, suggested by the base-line position of the schlieren pattern (zero gradient) between the peaks.

Table II: Limits of the Region of Monomer–Polymer Equilibrium and Size of Corresponding Polymer Species

muscle	pH	$s_{20,w}$	salt concn[a] at lower limit	salt concn[a] at upper limit
skeletal[b]	8.3	150	0.13	0.22
	6.8–7.1	180, 330, 1100	0.20	0.30
	6.2–6.8	330, 1100	0.20	0.35
smooth[c]	8	120	0.15	0.32
	7	200	0.18	0.35
	6	~500	0.25	>0.4

[a] Measured in mol/L KCl in 2 mM buffer, 4 °C. Values were interpolated between conditions where no monomer was detected (lower limit) and where no polymer was detected (upper limit). [b] Adapted from Josephs & Harrington (1966). [c] Buffer includes 1 mM EDTA and 0.5 mM DTT.

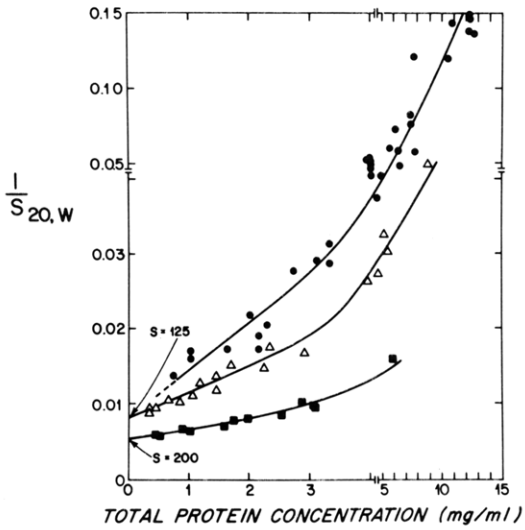

FIGURE 3: Sedimentation coefficient of myosin polymers as a function of total protein concentration at 20 °C: 0.2 M KCl, pH 7 (■) and 8 (△). In 0.25 M KCl, pH 8 (●), no polymer was visible below about 1 mg/mL because of the relatively low values of K_{eq} in this system. Note the concave upward curvature of the slope for this system at higher protein concentration, similarly observed with skeletal myosin (Josephs & Harrington, 1966). This curvature is real; both axes were foreshortened equally at the upper values to avoid graphical distortion of the slopes.

guished by the presence of distinct boundaries) when the pH is less than 7.5 (Josephs & Harrington, 1966).

(*2*) *Size and Morphology of Polymer.* The effect of pH on the size of the polymeric species formed is summarized in Figures 3–5. There is an increase in the sedimentation coefficient from 120 to 200 S on decreasing the pH from 8 to 7 (Figure 3), with a more pronounced increase to values in the range 250–800 S at pH 6 (not shown). A more accurate determination of the sedimentation coefficient at pH 6 was not possible due to the high variability of the data. Measurements taken from electron micrographs of negatively stained filaments prepared by dialysis in 0.2 M KCl (Figure 4) show there is a concomitant increase in filament diameter, from 100 Å at pH 8 to 225 Å at pH 6, although the filament length remains approximately constant, at 0.35 μm, regardless of pH (Figure 5A). The higher sedimentation rate at lower pH therefore reflects both an increase in molecular weight and a decrease in filament asymmetry. With a similar change in the pH from 8.3 to 7, the sedimentation coefficient of skeletal muscle myosin filaments increased only from 150 to 180 S (Josephs & Harrington, 1966). In these filaments, however, length rather than diameter is the dimension most sensitive

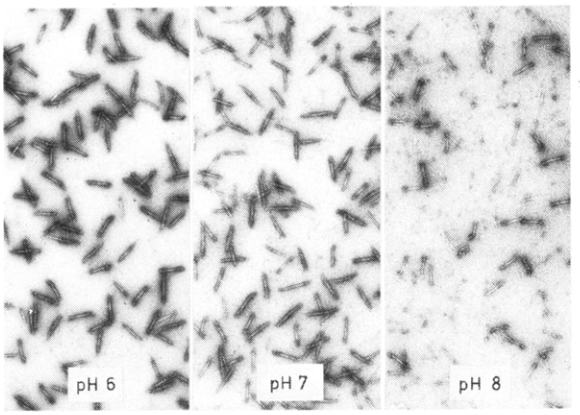

FIGURE 4: Electron micrographs of filaments of smooth muscle myosin formed by dialysis in 0.2 M KCl, pH 6, 7, or 8, in the presence of 1 mM EDTA, 0.5 mM DTT, and 2 mM phosphate (pH 6 and 7) or veronal (pH 8) buffer, 4 °C, at a total protein concentration of 3 mg/mL. Magnification, 8540×.

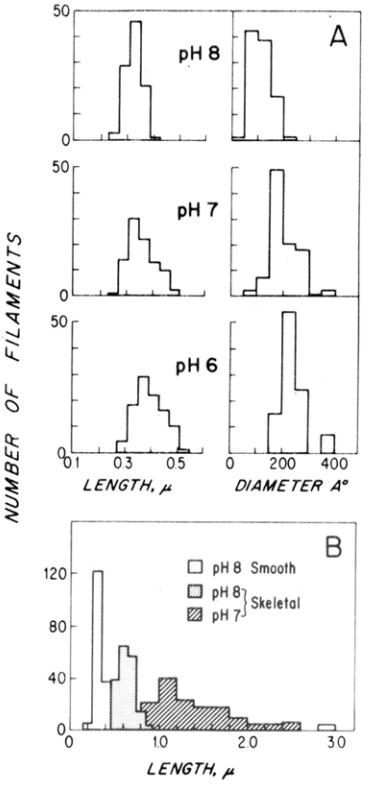

FIGURE 5: Histograms depicting the dimensions of filaments shown in Figure 4. (A) Length and diameter of smooth muscle filaments dialyzed in 0.2 M KCl, pH 6, 7, or 8. Although each histogram represents the distribution of more than 100 filaments, the ordinates were normalized to 100 filaments per histogram for purposes of comparison. (B) Comparison of 160 smooth muscle filaments formed at pH 8 [from part (A)] with skeletal muscle filaments formed at pH 7 and 8 [adapted from Josephs & Harrington (1966)]. Over 95% of skeletal muscle filaments formed at pH 6 were longer than 2 μm, and their distribution is not shown for simplicity. Note that on these axes smooth muscle filaments formed at pH 6 and 7 would nearly superimpose the pH 8 distribution.

to pH (Figure 5B), and the effect of increasing molecular weight on the sedimentation coefficient is somewhat counterbalanced by an increase in asymmetry.

At greater magnification, it becomes evident that the filaments produced at pH 6 and 8 can have significantly different structures (Figure 6). The filament produced at pH 8 is similar to the bipolar filament produced by skeletal muscle myosin in its initial stages of polymerization (Figure 6a).

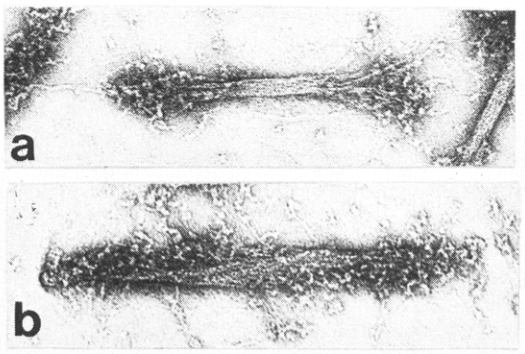

FIGURE 6: Enlargements of aorta myosin filaments formed in 0.2 M KCl, pH 7, photographed from the same grid. (a) Bipolar filaments, morphologically similar to the kind produced by skeletal muscle myosin; (b) side-polar filament with asymmetric "bare zones" that do not completely overlap, thus giving the filaments an oblique appearance. See Craig & Megerman (1977) for further details of filament morphology. Magnification, 209 600×.

However, it appears that the length of the smooth muscle myosin bipolar filament is limited to around 0.35 μm [Figure 5A; see also Kaminer (1969) and Shoenberg (1969)] whereas skeletal muscle filaments average 0.6 μm at pH 8 and achieve lengths greater than 6 μm at pH 6 (Josephs & Harrington, 1966). At the lower pH, smooth muscle myosin forms a side-polar structure which has the appearance, in projection, of an oblique parallelogram (Figure 6b). Larger filaments are formed by the addition of myosin molecules, or small oblique aggregates, parallel to the bare zones already present. It is the growth of this side-polar filament in its initial stage which gives rise to the observed increase in filament diameter, while filament length remains constant (Figure 5A). But the length of side-polar filaments is in fact more variable than that of the bipolar filament and is sensitive to the rate of polymerization. Thus, filaments can be as long as 6 μm when they are formed slowly in 0.3 M KCl, pH 6 (Craig & Megerman, 1977). The distribution of filaments between side-polar and bipolar structures is similarly affected by rates of polymerization, being sensitive to ionic strength, pH, and protein concentration, but not to the presence of divalent cations (Craig & Megerman, 1977). In 0.2 M KCl, the two types of filaments coexist in equal numbers at pH 6 and 7, while the bipolar filament predominates at pH 8. Because the distribution of filaments obtained at pH 8 was more consistent than those obtained at pH 6 and 7, the present study of monomer–polymer equilibria was limited to results obtained at pH 8.

(*3*) *Effects of Pressure.* As with skeletal muscle myosin, the equilibrium constant for polymerizing smooth muscle myosin is a sensitive function of pressure. This can readily be demonstrated by increasing the speed of rotation in the analytical centrifuge. Figure 7a shows the schlieren pattern obtained after the slow and fast boundaries have separated at 20 000 rpm. At constant speed, this pattern remains essentially unchanged except for the centrifugal motion of the two peaks, consistent with a stable equilibrium. When the rotational speed is suddenly increased to 60 000 rpm, however, the resultant increase in hydrostatic pressure shifts the equilibrium toward an increase in monomer concentration, and a substantial amount of protein depolymerizes. This newly created monomer (or small oligomer) forms a differential boundary which, because of its high local concentration, sediments more slowly than the normal "monomer" boundary (Figure 7b–d). The latter can thus catch up to the differential boundary, and with time the two boundaries merge into a single boundary with a sedimentation coefficient intermediate between those of the two separate boundaries (Josephs & Harrington, 1968).

Even at constant speed, the hydrostatic pressure increases with the radius within the centrifuge cell, though not as markedly as when the rotor speed is increased. Thus, as the polymer boundary traverses the cell to regions of greater pressure, increasingly greater concentrations of monomer are left behind. This is evidenced by the increase in the fringe count between the monomer and polymer boundaries, an observation used to estimate the change in the equilibrium constant, K, as a function of pressure (Josephs & Harrington, 1967, 1968). With the assumption that only two species exist (monomer and one polymer), whose molecular weights are known, K is related to the change in the partial specific volume, $\Delta\bar{v}$, due to polymerization from the monomer by eq 1 where

$$\log K = \log K_0 - \frac{nM\Delta\bar{v}}{2.3RT}(P_0 + P_r) \qquad (1)$$

r is the radius at any point within the cell, K is the equilibrium constant at that point, K_0 corresponds to the meniscus (r_0) where atmospheric pressure (P_0) is assumed, and

$$P_r = \frac{\rho\omega^2}{2}(r^2 - r_0^2)$$

or the increase in hydrostatic pressure within the cell, ρ is fluid density, ω is rotational speed, n is the number of monomers assumed to form the polymer, M is the molecular weight of the monomer, R is the universal gas constant, and T is the temperature. A plot of log K vs. r^2 should thus be linear, providing K_0 from the intercept and $\Delta\bar{v}$ from the slope (Figure 8). When the initial protein concentration is sufficiently high, the polymer boundary remains hypersharp throughout the centrifuge run (Figure 8, inset), and its location within the cell (r) can be precisely determined, as can the hydrostatic pressure at that point, the monomer concentration just centripetal to the polymer boundary (assumed to be in equilibrium

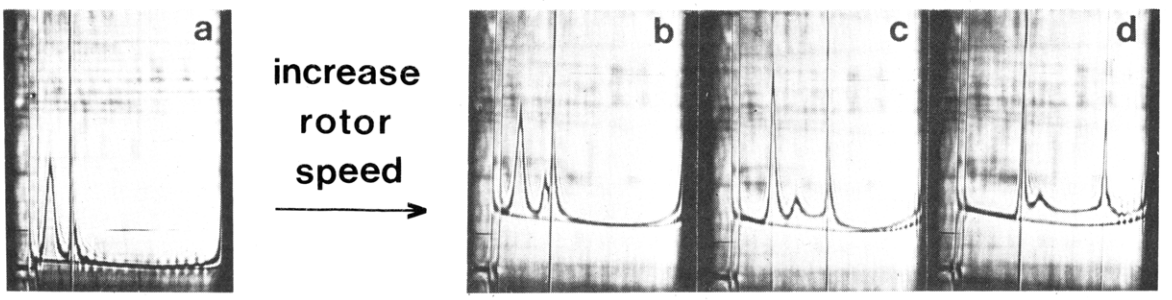

FIGURE 7: Effect of pressure on the stability of myosin polymer. After the establishment of a two-boundary system, at 20 000 rpm, the hydrostatic pressure was rapidly increased by raising the rotor speed to 60 000 rpm. The heavier species was partially depolymerized, causing the formation of the differential boundary which in time merged with the slowest boundary. Aorta myosin, 6 mg/mL, in 0.25 M KCl, pH 8, 5 °C. Bar angle 55°. Time (min) after attaining constant rotor speed: (a) 28, (b) 2, (c) 18, (d) 42.

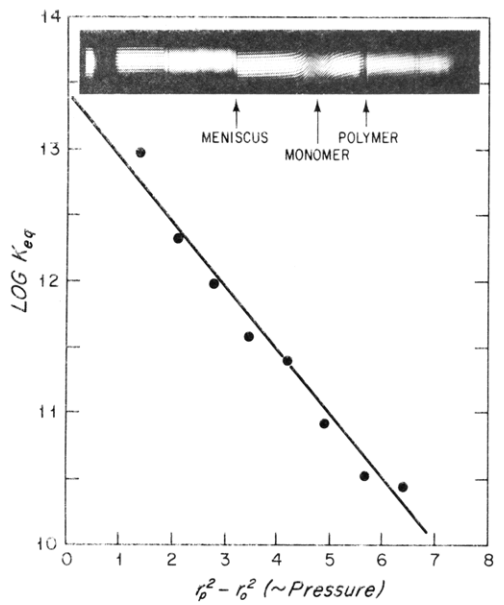

FIGURE 8: Effect of pressure on the apparent equilibrium constant, calculated from the monomer concentration near the polymer boundary at different times during a single constant velocity run, assuming two species only. The slope of the eye-fitted line was used to estimate $\Delta\bar{v}$. Aorta myosin, 12.4 mg/mL, in 0.25 M KCl, pH 8, 5 °C. Inset: Interference photograph taken after 9.5 h at 20 000 rpm. Note the clarity of the hypersharp polymer boundary which makes its position unambiguous, and the increasing monomer concentration between the two boundaries.

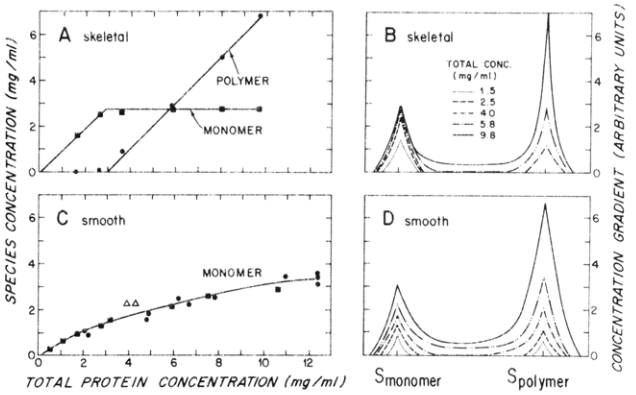

FIGURE 9: Effect of total myosin concentration on the distribution of fast (polymer) and slow (monomer) moving boundaries at 20 000 rpm, 5 °C. Note the presence of a relatively sharp "knee" in the monomer distribution of skeletal muscle myosin (A) which does not occur with smooth muscle myosin (C). In (C), different symbols represent different preparations of aorta myosin; the polymer distribution was omitted for reasons of clarity. (B and D) Schematic drawings of schlieren patterns that correspond to experiments depicted in (A) and (C), respectively. The abscissa represents the dimensionless "distance" between the two peaks observed within the centrifuge cell. The ordinate represents the shape of the schlieren pattern, where the height of each peak corresponds directly to the species concentration depicted in (A) or (C). Line symbols, representing different values of total concentration, apply equally to (B) and (D). Note that in (B) the area under the slower peak increases with total protein concentration until the critical concentration is reached [the "knee" in (A)] after which the faster moving peak appears and continues to grow while the slower peak remains unchanged. In (D), both boundaries are present at all but very low concentrations, and the two peaks grow simultaneously with increasing protein concentration. Skeletal muscle myosin in 0.19 M KCl, pH 8.3; smooth muscle myosin in 0.25 M KCl, pH 8.

with polymer), and the radial dilution correction factor.

Equation 1 was applied to data obtained at different times during a single sedimentation velocity run with aortic smooth muscle myosin. The polymer concentration was assumed to equal the total initial concentration minus that of the monomer, while n was estimated from electron micrographs. With the assumption that the polymer at pH 8 is a prolate ellipsoid of diameter 100 Å and length 3300 Å (Figure 5A), and with 0.728 cm^3/g as the partial specific volume, the molecular weight of polymer is approximately 14×10^6, or $n \simeq 28$. The corresponding sedimentation coefficient, using the above dimensions to estimate the frictional coefficient (Tanford, 1961), is 88 S, a value somewhat lower than the measured value of 120 S. Thus, $n = 30$ was used as a first approximation. K was calculated according to eq 4 below, and the results are shown in Figure 8. The slope of this linear plot gives $\Delta\bar{v} = 8.09 \times 10^{-4}$ cm^3/g, which is similar to the value of 6.4×10^{-4} cm^3/g obtained for skeletal muscle myosin (Josephs & Harrington, 1968). Note that calculations of $\Delta\bar{v}$ depend on the choice of n; choosing $n = 24$ would have made the values of $\Delta\bar{v}$ for the two myosin systems equal.

(4) Determination of Equilibrium Constant and Value of n. For a monomer–polymer system that contains only two species in equilibrium, eq 2–4 apply, where M and P are the

$$n = P/M \tag{2}$$

$$C_t = C_m + C_p \tag{3}$$

$$K = C_p/C_m^n \tag{4}$$

molecular weights of monomer and polymer and C_t, C_m, and C_p are the total and species concentrations (defined here by separated sedimenting boundaries). If the system is insensitive to pressure, or if equilibrium is achieved sufficiently rapidly after the rotor is accelerated, sedimentation velocity runs provide a convenient method for determining C_m, as well as C_p, by subtraction from C_t. A logarithmic representation of eq 4 then yields n as the slope of log C_p vs. log C_m and log K as the intercept at $C_m = 1$.

The above requirements are adequately met by the monomer–polymer system of skeletal muscle myosin at pH 8.3, as shown by Josephs & Harrington (1966, 1968), who calculated $K \sim 10^{50}$ (concentration was measured in units of g/100 mL), using the area under the schlieren peak to calculate C_m, and the value $n = 83$ obtained from viscosity and sedimentation data, in eq 4. Equation 4 was not used to calculate n because its large value precluded the determination of slope in the limited range covered by their data when it was plotted logarithmically. One consequence of the high value of n in a two-species system is that C_m increases with C_t only until a critical value is reached. Then C_m remains approximately constant for all higher values of C_t [Figure 13 in Josephs & Harrington (1966); Figure 9A]. In other words, a plot of C_m vs. C_t exhibits a sharp "knee" at the critical concentration. The schlieren patterns observed during velocity sedimentation runs of the skeletal myosin system are schematically summarized in Figure 9B. According to Gilbert (1955), for sufficiently large n, a sedimenting monomer–polymer system produces two well-separated peaks. Moreover, the more rapidly sedimenting peak (due to the polymer) is absent until the critical concentration is attained, while beyond that critical concentration the area under the more slowly sedimenting peak remains constant. Under the latter conditions, it can be shown (Josephs & Harrington, 1968) that this area corresponds closely to C_m.

When the monomer–polymer system for aorta myosin in 0.25 M KCl at pH 8 was studied by velocity sedimentation (Figure 9C), no critical concentration could be found beyond which C_m remained constant, despite total concentrations of up to 12 mg/mL. That is, the curve describing C_m vs. C_t did not exhibit a "knee", nor were the observed growths of the

monomer and polymer peaks consistent with predictions of the Gilbert theory for a two-species system. Although there appeared to be good separation between these peaks, the areas under both peaks increased together over nearly the entire range of total concentrations (Figure 9D). Furthermore, plotting log C_p vs. log C_m (eq 4) yielded an excellent linear correlation with $n = 2$, suggesting the polymer species was a dimer! While the value $n = 2$ is not precise, the data were sufficiently accurate to preclude the possibility that errors in determining the slope could account for this more than 10-fold divergence from the expected value. Similar results were obtained with aorta myosin in 0.25 M KCl, pH 7, and in 0.2 M KCl, pH 7 or 8. There was, thus, some question as to whether the conditions assumed when invoking the Gilbert theory did in fact exist. That theory presumes that a system is fully equilibrated, or that the rate of equilibration between species is much faster than the rate at which the different species are separated in the centrifuge. Factors related to the rate of equilibration of the monomer–polymer system were therefore further explored.

(5) *Equilibration and Reversibility.* To test the rate of depolymerization, two samples of smooth muscle myosin at 6 and 3 mg/mL were dialyzed overnight to 0.25 M KCl, pH 8. The more concentrated sample was rapidly diluted with buffer to arrive at the lower concentration. The samples were then immediately compared in the analytical ultracentrifuge where similar concentrations were observed for the slower peak. For the testing of rapid polymerization, a sample equilibrated in 0.5 M KCl, 4 mM veronal buffer, 2 mM EDTA, and 1 mM DTT, pH 8, was diluted with an equal volume of water to induce polymer formation. Immediate comparison with an equivalent sample that had been dialyzed to the same final conditions again gave identical results. Changes in equilibrium following a change in ionic conditions or total concentration thus appear to be rapid, but because of the time required to fill the centrifuge cells, mount the rotor, evacuate the chamber, and accelerate the rotor to 20000 rpm, we can at best conclude from these experiments that an equivalent state of equilibrium had been reached within 11 min of inducing the change.

The rate of equilibration during centrifugation, following changes induced by the application of pressure, was studied by using turbidity within the centrifuge cell as an index of the concentration of polymer at any point within the cell. The decrease in polymer concentration that occurs with increasing centrifugal pressure causes marked changes in turbidity as a function of the radius (Josephs & Harrington, 1967). The rapidity with which these profiles change is an indication of how fast a system is equilibrating. In separate runs, the turbidities of skeletal muscle myosin in 0.18 M KCl, pH 8.3, and smooth muscle myosin in 0.25 M KCl, pH 8, were continually recorded while the rotor was accelerated to 52000 rpm. After each of several designated speeds was attained, recordings were continued for several minutes to determine if any changes in polymer concentration were still occurring. Scanner optics were used, at wavelengths that limited the maximum absorption to 1 unit of optical density: 365 nm for skeletal muscle myosin and 305 nm for smooth muscle myosin. Both proteins exhibited marked changes in turbidity patterns following increases in rotor speed, as expected, though the changes obtained with aorta myosin were less pronounced. In all cases, turbidity patterns remained constant after at most 15 s of reaching desired speeds, suggesting that both systems were indeed equilibrating rapidly.

To test for a possible effect of temperature on the rate of equilibration during centrifugation, samples that had been polymerized by overnight dialysis at 4 °C (to minimize protein denaturation) were reequilibrated to 10, 15, or 20 °C, using the centrifuge's temperature control system, before accelerating the rotor. The results were not significantly different from those obtained at 4 °C. The similar absence of any temperature effect on the equilibrium distribution of monomer and polymer for skeletal muscle myosin has been reported (Josephs & Harrington, 1968).

We also considered the possibility that some protein was not available for reequilibration due to irreversible effects: that some monomer was "incompetent", or incapable of being polymerized, or that some polymer could no longer be depolymerized. We attempted to verify the absence of incompetent monomer by forming polymer from samples which might contain the greatest concentration of incompetent monomer. Monomer was isolated by centrifugation from the most concentrated sample of myosin equilibrated in 0.25 M KCl, pH 8 (12.4 mg/mL total concentration), and examined in the analytical centrifuge to verify the absence of polymer. The sample was then concentrated to 7.85 mg/mL by dialysis against buffer containing 6% (w/v) poly(ethylene glycol) 6000 to reduce the sample volume. When reexamined in the analytical centrifuge, the measured concentration under the slow peak (3.15 mg/mL) was sufficiently close to the value expected (Figure 9C, solid line) to conclude that less than 7% of the original (12.4 mg/mL) protein was incompetent.

The amount of polymer that could not reversibly depolymerize was estimated by comparing the monomer concentration obtained following depolymerization of a concentrated sample of polymer with that obtained by the usual dialysis of monomer to low ionic strength. Concentrated samples of myosin in 0.25 M KCl, pH 8, were diluted with buffer to one-third and one-sixth of their initial concentration and brought to 20000 rpm in the analytical centrifuge as quickly as possible. These initial and final concentrations were chosen in an effort to induce as large a measurable change in monomer concentration as possible. The measured values of final concentration under the slow peak were significantly greater than those that would have resulted if there had been no reequilibration, but they were also less than expected. Thus, about 50% of the polymer had failed to depolymerize completely after dilution by the time the speed of centrifugation had been reached.

(6) *Equilibration at Constant Pressure.* To avoid the possible influence of changing hydrostatic pressure on the observed monomer–polymer equilibrium distribution, we measured the amount of 90° light scattering (Wegner, 1976) under conditions of constant (atmospheric) pressure. Equilibrated solutions of monomer and polymer were prepared as before by dialysis to final conditions at 4 °C, and large particulates were removed by centrifugation at 10000 rpm for 20 min. The supernatant was placed in an optical cuvette and left in the spectrophotometer to equilibrate to 10 °C, the lowest temperature that was technically convenient.

The method was first tested with skeletal muscle myosin at pH 8.3, for which the results are shown in Figure 10A. The amount of scattered light varied linearly with protein concentration for monomer in 0.6 M KCl, and for monomer-free polymer in 0.12 M KCl. The amount of scattering due to polymer was 60-fold greater than that for monomer, a ratio not too different from the anticipated ratio of their molecular weights ($n = 83$). In 0.19 M KCl, a pronounced "knee" was observed: little scattering occurred until a critical total concentration was attained, beyond which the amount of scattering increased sharply. The corresponding experiment with aorta

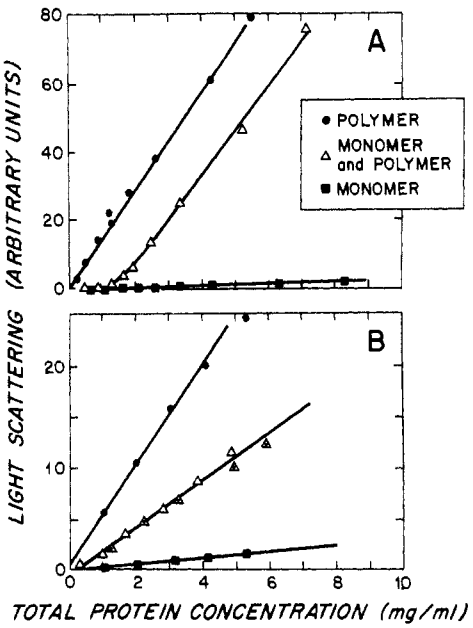

FIGURE 10: Light scattering at 90° and 600 nm by myosin systems in equilibrium, as a function of total protein concentration at 10 °C. Note the use of different vertical scales necessitated by the differences in the amount of scattering by the two types of polymer. Scattering values for monomer are identical for the two myosins. (A) Skeletal myosin at pH 8.3 in 0.12, 0.19, and 0.6 M KCl. Note, as in Figure 9A, the presence of a "knee" in the monomer–polymer system. (B) Aorta myosin at pH 8 in 0.13, 0.25, and 0.6 M KCl.

myosin at pH 8 is summarized in Figure 10B. The light scattered by monomer in 0.6 M KCl, by polymer in 0.13 M KCl, and by the two in equilibrium in 0.25 M KCl *all* varied linearly with concentration. The results for monomer were identical with those obtained with skeletal myosin monomer, though for polymer, the sensitivity was only 18-fold greater, as might be expected for the smaller polymer. For the mixture, the slope was midway between those obtained for the pure components, and the data showed no evidence for the existence of a critical concentration.

Discussion

Based on our limited physical characterization of monomeric calf aorta myosin, we find it to be very similar to other vertebrate smooth muscle myosins. Even when compared to myosin from rabbit skeletal muscle, aortic myosin seems to differ in only minor respects. The myosins from the two types of muscle are different in light chain composition, but they have similar molecular weights, and measured viscosities were within limits of experimental error. They also sediment identically when they are centrifuged simultaneously, a procedure which eliminates possible differences in temperature between separate runs.

The amino acid composition of the several myosins was also similar, despite differences in the source of the myosins and methods of purification. On the average, the smooth muscle myosins contained a significantly greater content of Glx, Leu, and Arg, with less Pro, Val, Ile, and Tyr compared with skeletal myosin. This lower Tyr content is consistent with the lower extinction coefficient we found for aortic myosin. Differences in the compositions of smooth muscle myosins (e.g., hog and calf aorta myosins) are most likely due to species differences or to experimental error, although the mode of extraction (e.g., low vs. high ionic strength) coupled with the possible presence of isoenzymes (Hamoir & Laszt, 1962) may account for some differences.

Comparison of Myosin Polymers. Despite the numerous similarities that exist between the myosins of smooth and skeletal muscle, significant differences become evident when the two proteins are polymerized in vitro by lowering the ionic strength. The study of filament formation may thus be a sensitive means for comparing different myosins. When smooth muscle myosin polymerizes in vitro, it forms either bipolar or side-polar filaments. However, this polymorphism is not due to the presence of different myosins, and the type of filament formed depends on the rate of polymerization (Craig & Megerman, 1977). It has been suggested that smooth muscle myosin forms only side-polar filaments and that the bipolar filament we observe is in fact a short side-polar filament that is viewed accidentally from an angle that masks the symmetrical bare zones, resulting in only the appearance of a central bare zone (Hinssen et al., 1978). Our observation of the distribution of side-polar and bipolar filaments under varying conditions of polymerization makes this explanation unlikely. At pH 6 and 7, the two types of filament were distributed in approximately equal amounts. At pH 8, however, bipolar filaments were seen predominantly. If the visualization of bipolar filaments depended on their accidental orientation on the microscope grid, then more side-polar filaments should have been visible at pH 8. In addition, the incorporation of smooth muscle myosin into bipolar filaments composed mostly of skeletal muscle myosin (Pollard, 1975; Kaminer et al., 1976) suggests that smooth muscle myosin is itself capable of forming bipolar filaments. The size of this bipolar filament seems to be limited to about 0.35 μm in length. Based on its appearance in the electron microscope, its sedimentation coefficient, and the amount of light it scatters, we estimate this filament to be composed of 20–40 monomers, or less than half the number that make up skeletal myosin filaments under similar conditions.

Comparison of Equilibrium Distributions. The relationship between monomer and polymer in smooth muscle myosin also differs significantly from that which occurs with skeletal muscle myosin, despite the many similarities that exist between the two polymerization systems. The manner in which the monomer concentration changes as a function of the total concentration of smooth muscle myosin (Figure 9C) is too unlike that obtained with skeletal myosin to consider the mechanisms of polymerization for the two myosins to be equivalent. The polymerization of skeletal myosin is consistent with the Gilbert theory, which predicts the appearance of a fast moving boundary only after the slower boundary has reached a maximum "critical" concentration. For aorta myosin, however, polymer is present even at very low total protein concentrations, while no reasonable concentration exists beyond which the concentration of the slow peak remains nearly constant.

This difference between the shapes of Figure 9A and C appears to be more than a simple artifact. Possible errors in experimental technique were checked by repeating the experiments with skeletal muscle myosin and comparing the results with published data. The results shown in Figure 9A are similar to those of Josephs & Harrington (1966), although ionic conditions were slightly different. The calculated equilibrium constant (at 20 000 rpm, $P \simeq 5$ atmospheres, assuming $n = 83$ and expressing concentrations in weight units, g/100 mL) is $K = 10^{45}$, which lies within the range of expected values (Josephs & Harrington, 1968, Figure 5). The possible influence of variations in preparative procedures and the lack of reversibility or equilibration were also examined and seem to be improbable causes of the observed differences relating

to the existence of a critical concentration.

The problems associated with changes in equilibrium during rotor acceleration were avoided by studying a constant-pressure system by means of light scattering (Figure 10). The method was again tested by using skeletal muscle myosin under known conditions. Since light scattering is proportional to the weight-average molecular weight in a mixture of macromolecules, the method is most sensitive to polymer concentration even in a mixture with monomer. Therefore, we conclude that little or no polymer was formed below 1.5 mg/mL total protein, while at greater concentrations, the nearly parallel slopes observed for pure polymer and for the heterogeneous mixture suggest that all added protein was converted to polymer exclusively. In other words, C_m remained constant beyond the critical concentration, as had been observed in the analytical centrifuge. The parallel slopes also suggest that the polymers formed in 0.19 and 0.12 M KCl are of equal size or that they are both sufficiently large to render light scattering insensitive to changes in polymer length (Gaskin et al., 1974). Despite the qualitative nature of these data, an average equilibrium constant was calculated, using $n = 83$ and eq 3 and 4. The value $K = 10^{64}$ is again near that obtained from the data of Josephs & Harrington (1968). The use of 90° scattering to analyze the distribution of monomer and polymer in equilibrated solutions of myosin therefore seems justified.

The results obtained with smooth muscle myosin (Figure 10B), while difficult to interpret, at least support the hypothesis that the polymerization processes of smooth and skeletal muscle myosins are different. Although the lower amount of light scattered in 0.25 M KCl, compared with 0.13 M KCl, could be due to the formation of a smaller polymer at the higher salt concentration, this difference in size alone could not account for the absence of a sharp change in slope that must occur if eq 2–4 apply.

The straightforward description of the equilibrium distribution of polymerizing skeletal muscle myosin (Josephs & Harrington, 1966) resulted from the large values of the equilibrium constant, K, and the number of monomers per polymer, n. These provide for a clear separation of two sedimenting boundaries and enable the slow and fast boundaries to be identified primarily with monomer and polymer, respectively, in accordance with Gilbert's theory (Gilbert, 1955; Josephs & Harrington, 1968). Our inability to apply this simple analysis to smooth muscle myosin could result in part from the much smaller size of the polymer ($n \lesssim 30$) and equilibrium constant ($K \simeq 10^{13}$), which we calculated on the basis of a two-species model. The effect of diffusion, which is not considered by the Gilbert theory, could also be a significant factor with smaller oligomers. Moreover, if different kinds of bonds of unequal energy are present in a rapidly reversible system, a discrete number of intermediate-sized species might be formed, which could escape detection by ultracentrifugation. The simultaneous presence of bipolar and side-polar filaments supports this possibility.

Since this work was completed, the effect of phosphorylation on the assembly and disassembly of smooth muscle myosin has been reported (Suzuki et al., 1978; Scholey et al., 1980). These investigators have shown that the state of phosphorylation of myosin can have a strong influence on the stability of its filaments in millimolar concentrations of MgATP. Although our polymerization medium contained no MgATP, it is nevertheless possible that the largely unphosphorylated state of our myosin (based on the complete lack of actin-activated ATPase activity) might have contributed to some of the unusual features of the myosin–polymer equilibrium. Further studies comparing the polymerization of phosphorylated and unphosphorylated myosins are clearly needed to resolve the exact nature of the differences between the self-association of skeletal and smooth muscle myosins.

References

Aksoy, M. O., Williams, D., Sharkey, E. M., & Hartshorne, D. J. (1976) *Biochem. Biophys. Res. Commun. 69*, 35–41.

Ashton, F. T., Somlyo, A. V., & Somlyo, A. P. (1975) *J. Mol. Biol. 98*, 17–29.

Bârâny, M., Bârâny, K., Gaetjens, E., & Bailin, G. (1966) *Arch. Biochem. Biophys. 113*, 205–221.

Bremel, R. D. (1974) *Nature (London) 252*, 405–407.

Chacko, S., Conti, M. A., & Adelstein, R. S. (1977) *Proc. Natl. Acad. Sci. U.S.A. 74*, 129–133.

Cohen, C., Lowey, S., & Kucera, J. (1961) *J. Biol. Chem. 236*, 23–24.

Craig, R., & Megerman, J. (1977) *J. Cell Biol. 75*, 990–996.

Dabrowska, R., Sherry, J. M. F., & Hartshorne, D. J. (1979) in *Motility in Cell Function* (Pepe, F. A., Sanger, J. W., & Nachmias, V. T., Eds.) pp 147–160, Academic Press, New York.

DeRosier, D. J., Munk, T., & Cox, D. J. (1972) *Anal. Biochem. 50*, 139–153.

Ebashi, S., Endo, M., & Ohtsuki, I. (1969) *Q. Rev. Biophys. 2*, 351–384.

Fiske, C. H., & Subbarow, Y. (1925) *J. Biol. Chem. 66*, 375–400.

Frederiksen, D. W. (1979) *Biochemistry 18*, 1651–1656.

Gaskin, F., Cantor, C. R., & Shelanski, M. L. (1974) *J. Mol. Biol. 89*, 737–758.

Gilbert, G. A. (1955) *Discuss. Faraday Soc. 20*, 68.

Godfrey, J. E., & Harrington, W. F. (1970) *Biochemistry 9*, 894–908.

Gornall, A. G., Bardawill, C. J., & David, M. M. (1949) *J. Biol. Chem. 177*, 751–766.

Gröschel-Stewart, U. (1971) *Biochim. Biophys. Acta 229*, 322–334.

Hamoir, G., & Laszt, L. (1962) *Nature (London) 193*, 682–684.

Hamoir, G., & Gaspar-Godfroid, A. (1964) *Angiologica 1*, 317–337.

Hanson, J., & Lowy, J. (1964) *Proc. R. Soc. London, Ser. B 160*, 523–524.

Hinssen, H., D'Haese, J., Small, J. V., & Sobieszek, A. (1978) *J. Ultrastruct. Res. 64*, 282–302.

Holtzer, A., & Lowey, S. (1959) *J. Am. Chem. Soc. 81*, 1370–1377.

Huriaux, F. (1965) *Angiologica 2*, 153–181.

Huriaux, F., Pechere, J. F., & Hamoir, G. (1965) *Angiologica 2*, 15–43.

Huxley, H. E. (1963) *J. Mol. Biol. 7*, 281–308.

Huxley, H. E. (1969) *Science (Washington, D.C.) 164*, 1356–1366.

Josephs, R., & Harrington, W. F. (1966) *Biochemistry 5*, 3474–3487.

Josephs, R., & Harrington, W. F. (1967) *Proc. Natl. Acad. Sci. U.S.A. 58*, 1587–1594.

Josephs, R., & Harrington, W. F. (1968) *Biochemistry 8*, 2834–2847.

Kaminer, B. (1969) *J. Mol. Biol. 39*, 257–264.

Kaminer, B., & Bell, A. L. (1966) *J. Mol. Biol. 20*, 391–401.

Kaminer, B., Szonyi, E., & Belcher, C. D. (1976) *J. Mol. Biol. 100*, 379–386.

Lowey, S., & Cohen, C. (1962) *J. Mol. Biol. 4*, 293–308.

Lowey, S., & Risby, D. (1971) *Nature (London) 234*, 81–85.

Lowey, S., Slayter, H. S., Weeds, A., & Baker, H. (1969) *J. Mol. Biol. 32*, 1–29.
Megerman, J. (1974) Ph.D. Dissertation, University of Virginia, University Microfilms.
Megerman, J., & Murphy, R. A. (1975) *Biochim. Biophys. Acta 412*, 241–255.
Murphy, R. A., & Megerman, J. (1977) in *The Biochemistry of Smooth Muscle* (Stephens, N. L., Ed.) pp 473–498, University Park Press, Baltimore, MD.
Needham, D. M. (1971) *Machina Carnis: The Biochemistry of Muscular Contractions in Its Historical Development*, pp 545–577, Cambridge University Press, New York.
Pollard, T. D. (1975) *J. Cell Biol. 67*, 93–104.
Potter, J. D. (1974) *Arch. Biochem. Biophys. 162*, 436–441.
Richards, E. G., Chung, C. S., Menzel, D. B., & Olcott, H. S. (1967) *Biochemistry 6*, 528–540.
Roark, D., & Yphantis, D. A. (1969) *Ann. N.Y. Acad. Sci. 164*, 245–278.
Ruegg, J. C. (1971) *Physiol. Rev. 51*, 201–248.
Scholey, J. M., Taylor, K. A., & Kendrick-Jones, J. (1980) *Nature (London) 287*, 233–235.
Shoenberg, C. F. (1969) *Tissue Cell 1*, 83–96.
Small, J. V., & Squire, J. M. (1972) *J. Mol. Biol. 67*, 117–149.
Sobieszek, A. (1972) *J. Mol. Biol. 70*, 741–744.
Sobieszek, A. (1977) in *The Biochemistry of Smooth Muscle* (Stephens, N. L., Ed.) pp 413–443, University Park Press, Baltimore, MD.
Sobieszek, A., & Small, J. V. (1972) *Cold Spring Harbor Symp. Quant. Biol. 37*, 109–111.
Sobieszek, A., & Small, J. V. (1976) *J. Mol. Biol. 102*, 75–92.
Somlyo, A. V., Ashton, F. T., Lemanski, L. F., Vallières, J., & Somlyo, A. P. (1977) in *The Biochemistry of Smooth Muscle* (Stephens, N. L., Ed.) pp 445–469, University Park Press, Baltimore, MD.
Spudich, J. A., & Watt, S. (1971) *J. Biol. Chem. 246*, 4866–4871.
Suzuki, H., Omishi, H., Takahashi, K., & Watanabe, S. (1978) *J. Biochem. (Tokyo) 84*, 1529–1542.
Tanford, C. (1961) *Physical Chemistry of Macromolecules*, Wiley, New York.
Tregear, R. T., & Squire, J. M. (1973) *J. Mol. Biol. 77*, 279–290.
Wachsberger, P., & Kaldor, G. (1971) *Arch. Biochem. Biophys. 143*, 127–137.
Wachsberger, P. R., & Pepe, F. A. (1974) *J. Mol. Biol. 88*, 385–391.
Weber, K., & Osborn, M. J. (1969) *J. Biol. Chem. 244*, 4406–4412.
Wegner, A. (1976) *J. Mol. Biol. 108*, 139–150.
Yamaguchi, M., Miyazawa, Y., & Sekine, T. (1970) *Biochim. Biophys. Acta 216*, 411–421.

Proteolytic Approach to Structure and Function of Actin Recognition Site in Myosin Heads†

Dominique Mornet, Raoul Bertrand, Pierre Pantel, Etienne Audemard, and Ridha Kassab*

ABSTRACT: The protective effect of actin against tryptic cleavage of subfragment 1 (S1) heavy chain at the joint connecting the 75K and 20K peptides and against the resulting loss of acto-S1 Mg^{2+}–ATPase activity [Mornet, D., Pantel, P., Audemard, E., & Kassab, R. (1979) *Biochem. Biophys. Res. Commun. 89*, 925] is exercised not only on free S1 but also on the intact myosin. Mg^{2+}ATP and Mg^{2+}ADP impair the protective action of actin to an extent closely related to their respective affinities for the acto-S1 complex. Tryptic fragmentation of S1 heavy chain using trypsin to S1 weight ratios in the range 1:1000–1:1500 indicated that peptide bond cleavage at the 75K–20K joint is a sequential process giving rise first to a 22K peptide intermediate which is subsequently converted into the stable 20K fragment. Most importantly, it is also demonstrated that the loss of S1 activation by actin is not due to the initial scission of the 75K–22K linkage but is intimately associated with the breakdown of the 22K precursor into its 20K moiety. A detailed analysis of the C termini of three trypsin-modified S1 derivatives and of their isolated heavy chain fragments indicated that the 20K fragment is formed mainly through the degradation of an NH_2-terminal 2K segment in the 22K precursor and that this proteolytic event is the only one accounting for the acto-S1 ATPase loss. Cross-linking experiments exploiting the reaction of a carbodiimide reagent with rigor complexes containing either fluorescent actin or fluorescent fragmented S1 revealed unequivocally the attachment of actin monomer to recognition sites on the 20K and 50K units of S1 heavy chain.

The interaction of actin with myosin heads and the actin-dependent activation of the Mg^{2+}–ATPase[1] of the myosin molecule are crucial events of the mechanochemical transduction process in muscle and other motile systems. Whereas the kinetic parameters of the myosin and actomyosin mechanisms have been the subject of extensive research effort in recent years, our knowledge of their structural aspect remains essentially poor. In particular, little of the work on myosin has focussed on the nature and structure of actin recognition

† From the Centre de Recherches de Biochimie Macromoléculaire du Centre National de la Recherche Scientifique, Montpellier, France. *Received June 23, 1980; revised manuscript received November 5, 1980.* This research was supported by grants from Centre National de la Recherche Scientifique and Délégation Générale à la Recherche Scientifique et Technique (Action Concertée No. 76.7.I865).

[1] Abbreviations used: ATPase, adenosine 5′-triphosphatase (EC 3.6.1.3); S1, subfragment 1; acto-S1, actomyosin S1; A1, alkali light chain 1; A2, alkali light chain 2; $NaDodSO_4$, sodium dodecyl sulfate; ATP, adenosine triphosphate; ADP, adenosine diphosphate; PP_i, pyrophosphate; EDC, 1-ethyl-3-[3-(dimethylamino)propyl]carbodiimide; Tris, 2-amino-2-(hydroxymethyl)-1,3-propanediol; HMM, heavy meromyosin; LMM, light meromyosin.

0006-2960/81/0420-2110$01.25/0 © 1981 American Chemical Society